



Hydrogeological processes and geological settings over Europe controlling dissolved geogenic and anthropogenic elements in groundwater of relevance to human health and the status of dependent ecosystem

**Deliverable 4.3**  
**The use of microbial diversity measures for monitoring contaminant transforming processes at GW-SW transition zones**

Authors and affiliation:  
**Jennifer Hellal, BRGM**

**Tina B Bech, GEUS**

**Jens Aamand, GEUS**

E-mail of lead author:  
**j.hellal@brgm.fr**

Version: 25-10-2021

This report is part of a project that has received funding by the European Union's Horizon 2020 research and innovation programme under grant agreement number 731166.



<b>Deliverable Data</b>		
<b>Deliverable number</b>	D4.3	
<b>Dissemination level</b>	Public	
<b>Deliverable name</b>	Supporting documents	
<b>Work package</b>	WP4	
<b>Lead WP/Deliverable beneficiary</b>	Jens Aamand	
<b>Deliverable status</b>		
<b>Submitted (Author(s))</b>	20/10/2021	Jennifer Hellal, Tina Bech
<b>Verified (WP leader)</b>	22/10/2021	Jens Aamand
<b>Approved (Coordinator)</b>	30/10/2021	Laurence Gourcy





## TABLE OF CONTENTS

1	INTRODUCTION .....	2
2	SITE OVERVIEW .....	3
2.1	River Crieu.....	3
2.2	Risby stream .....	4
2.3	Holtum Stream.....	5
2.4	Planned work at each site.....	7
3	BACTERIAL DIVERSITY IN TRANSITIONS ZONES – LINK TO BIODEGRADATION OF PESTICIDES ..	8
3.1	Sequencing and data analysis.....	8
3.1.1	DNA extraction.....	8
3.1.2	16S Quantification .....	8
3.1.3	Amplicon Sequencing.....	8
3.1.4	Bioinformatics.....	8
3.1.5	Statistical Analyses.....	9
3.2	River Crieu.....	9
3.2.1	Water chemistry .....	9
3.2.2	Microbial diversity analysis.....	10
3.3	Risby stream .....	12
3.3.1	Diversity analysis.....	12
3.3.2	Evolution of diversity profiles after 100 days incubation .....	15
3.4	Holtum stream.....	17
3.4.1	Water chemistry .....	17
3.4.2	Diversity analysis.....	17
4	DISCUSSION – LINKING DIVERSITY AND DEGRADATION RATES IN SEDIMENT TRANSITION ZONES .....	21
4.1.1	Sediment diversity and DT50 for MCPA, metolachlor and propiconazole .....	21
4.1.2	Sediment diversity and degradation of antibiotics and two other pesticides, metamitron and parastrobins, in the Holtum stream sediments .....	22
4.1.3	Conclusion.....	23
5	REFERENCES.....	24



## 1 INTRODUCTION

Microbial diversity in the environment is driven by a multitude of factors including physico-chemical conditions such as pH, redox conditions, salinity, light, organic matter, etc. Generally, the great heterogeneity combined with the association of bacterial assemblages in biofilms leads to a great taxonomical and functional diversity in the hyporheic zone (Storey et al. 1999). Distinct gradients of dissolved oxygen, nutrient availability, and the presence of specific redox conditions vertically through this zone, lead to differences among microbial communities. The overall bacterial density was shown to vary greatly but seems to generally decrease with increasing depths along vertical flow paths (Sobczak & Findlay 2002). Other studies focusing on the association of biodegradation and bacterial diversity reported a close link of increased degradation potential with higher microbial diversity (Posselt et al. 2020).

In sediment within the hyporheic zone, located at the interface between a continuous water flow and the underlying sediment, the bacterial communities and their activity contribute to many biogeochemical cycles such as organic matter turnover, nitrate and phosphate cycling, and, depending on the anthropic pressure from agricultural or urban activities, they could play an important role in the degradation of organic pollutants.

Water quality management is more and more faced with compounds of emerging concern including pesticides, fungicides and pharmaceuticals, molecules that ends up in our surface and groundwater. At the interface between ground and surface water, stream and river sediments are thus exposed to these compounds which could impact the microbial communities present but also favour the enrichment of bacteria capable of degrading some of these persistent compounds.

Work package 4 of the GeoERA HOVER project aimed to investigate the degradation potential of the bacterial communities in sediments collected from 3 sites situated in France (Crieu River) and Denmark (Risby landfill and Holtum stream), susceptible to be impacted by several compounds due to agricultural and urban activities. The first deliverable, D4.1 presents these sites, D4.2. presents the degradation kinetic results for 5 compounds, four herbicides; 2-methyl-4-chlorophenoxyacetic acid (MCPA), metolachlor, metamitrone and pyraclostrobin, one fungicide, propiconazole and two antibiotics, sulfadiazine and sulfamethoxazole, while the present deliverable, D4.3. presents the bacterial diversity found in the sediment samples from the 3 sites and discusses them in relation to the degradation results, in particular to the dissipation time, DT50 (the time for 50% reduction of the contaminant).



## 2 SITE OVERVIEW

The main objective of WP4 is to increase our understanding of how groundwater ecology and microbial diversity determine contaminant-transforming processes at European groundwater-surface water (GW-SW) transition zones (hyporheic zones). To do this, three field sites were selected, two in Denmark and one in France. In common for the three sites is a solid knowledge of hydraulic heads and conductivities and, to some extent, knowledge of existing pollutants in the areas. The site in France and the Holtum stream in Denmark are impacted by agriculture, whereas the Risby site in Denmark is located near a landfill. Both situations are relevant to increase our knowledge on the degradation of contaminants in the hyporheic zone within streams. Detailed information on the French site and the landfill impacted Danish site can be found in Deliverable D4.1. This deliverable also contains information on a Latvian site that was abandoned due to travel restrictions resulting from the covid 19 pandemic. Instead, another Danish location (The Holtum stream) was selected for the research. Below, a short description of each of the three sites is given.

### 2.1 River Crieu

The study site in France is located in the alluvial plain of the Ariège River Basin, on the Crieu River (Figure 1). The alluvium was deposited in five distinct terraces of somewhat similar composition. The aquifer is unconfined, and the unsaturated zone is generally <10m thick. The alluvial plain is mostly cultivated farmland, mainly corn. This basin has been studied previously, which enabled us to choose locations along the river.

The main pesticides found in the groundwater along this river basin are (S-)metolachlor and, to a lesser extent, atrazine that was withdrawn from the market in 2003. Besides pesticides, also metabolites of pesticides (notably chloroacetanilides) have been found previously in high amounts (Amalric et al. 2013).

The study points for groundwater identified for the HOVER project are located in the middle and downstream stretches of the Crieu River. The infiltration of river water characterizes the first, Villeneuve du Paréage (Pz Vill), into the aquifer below. In contrast, the downstream site, Saverdun (Pz Sav), is characterized by an upwelling of groundwater towards the river (Figure 1). Samples for stream water and sediment analyses (chemistry, degradation potential and diversity) were collected from 6 points along the river section (CP3, CP4, CP5, CP6, CP6b and CP7) (Figure 1).

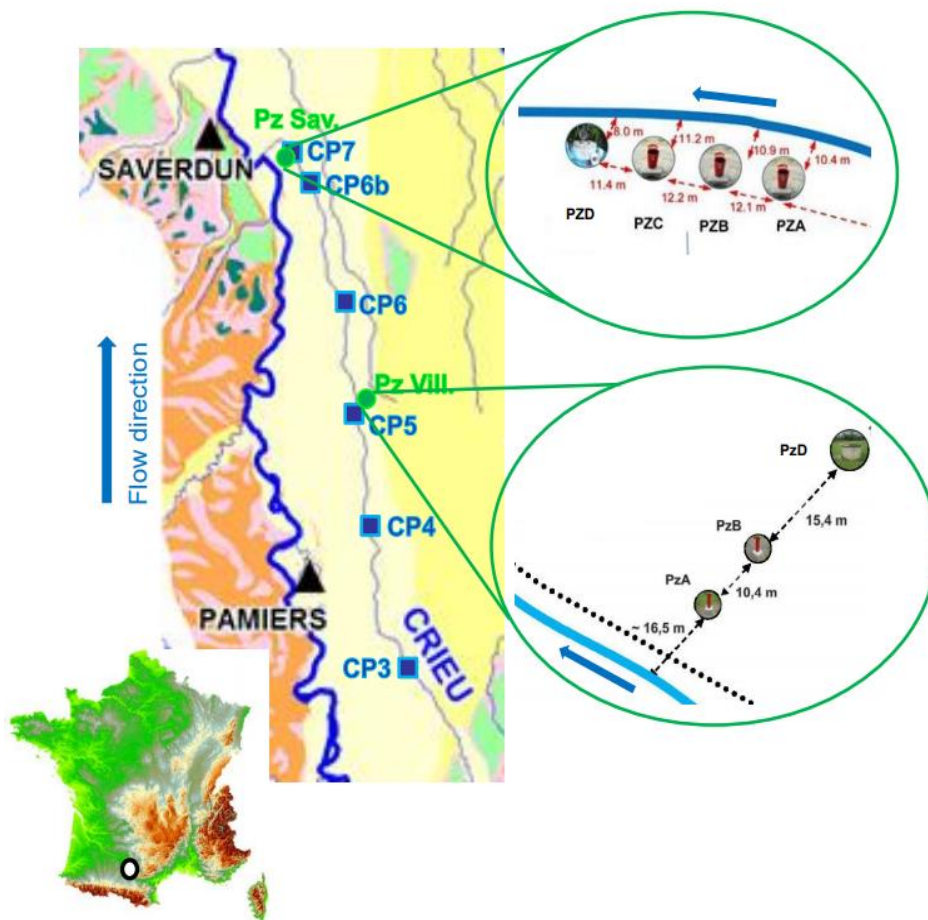


Figure 1. Localization of the Crieu River and the sampling spots identified for HOVER.

## 2.2 Risby stream

The Risby Landfill is located west of Copenhagen and was actively used from 1959 to 1981. It covers an area of 6.5 ha and contains a total of 500,000 m<sup>3</sup> of waste. There are no liners or leachate collection systems installed at the landfill. Although no detailed records exist, it contains a mixture of municipal waste, demolition waste, fly ashes, and some chemical waste. The potential for pesticide degradation in the hyporheic zone of the Risby stream has been studied previously where it was shown that locations with the highest mass discharge of pesticide had the highest degradation potentials (Batioğlu-Pazarbaşı et al. 2013). The groundwater flow direction from the landfill is towards the stream with varying water discharge volumes, as seen in Figure 2.

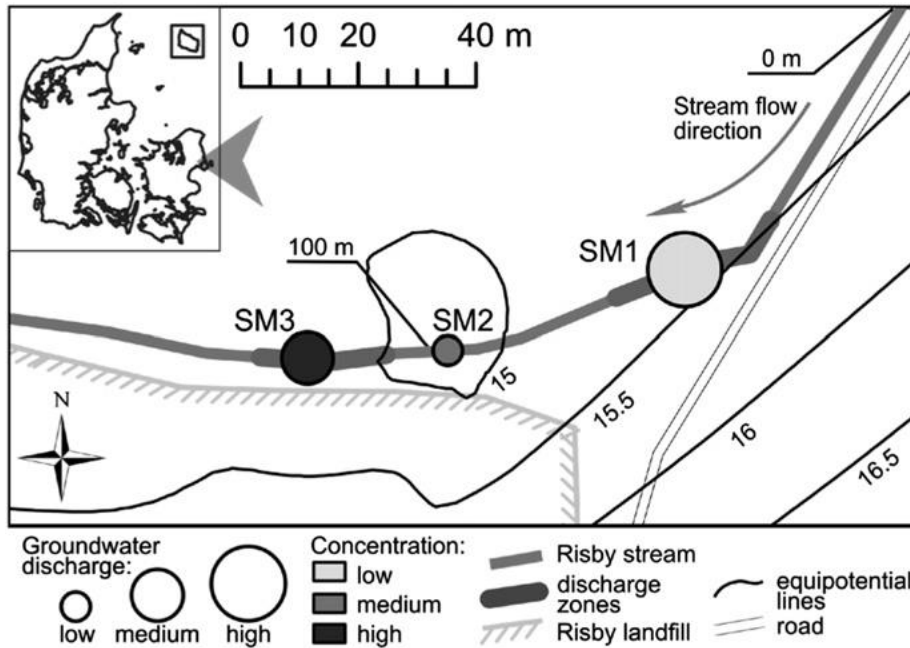


Figure 2. Sampling locations of the Risby Landfill and groundwater discharge zones. Groundwater was collected from the three seepage meters (SM1, SM2, SM3), and streambed sediments were collected in the vicinity of the SM. Sampled discharge zones have different pesticide mass discharges due to variations in the groundwater discharge and pesticide concentration (Batioğlu-Pazarbaşı et al. 2013). SM4 was sampled 100 m upstream from SM1.

### 2.3 Holtum Stream

The study was conducted in the groundwater-gaining lowland Holtum stream, located in the Skjern river catchment in Jutland, western Denmark (Fig. 1a). This glacial floodplain valley is characterized by thick sediment deposits of sand and silt deposited during the latest Weichsel glacial period (Houmark-Nielsen 1989), and with podzols being the dominating soil layers.

Between stations 1 and 4, the stream flows from east to west with a mean gradient of 1 ‰. Beyond a riparian zone of approximately 5 m, station 1 is surrounded by agricultural fields, whereas the near-stream areas at stations 2, 3 and 4 are wetlands. The mean annual discharge, the topographical catchment and land use of sub-catchments to each station are summarized in Table 1.

The main objective of the Holtum sampling was to compare the transformation of organic pollutants at station 1 (agricultural) and station 4 (natural) in the upper and lower sediment from the hyporheic zone and compare these transformations to the abundance and diversity of the bacterial community (Figure 3).

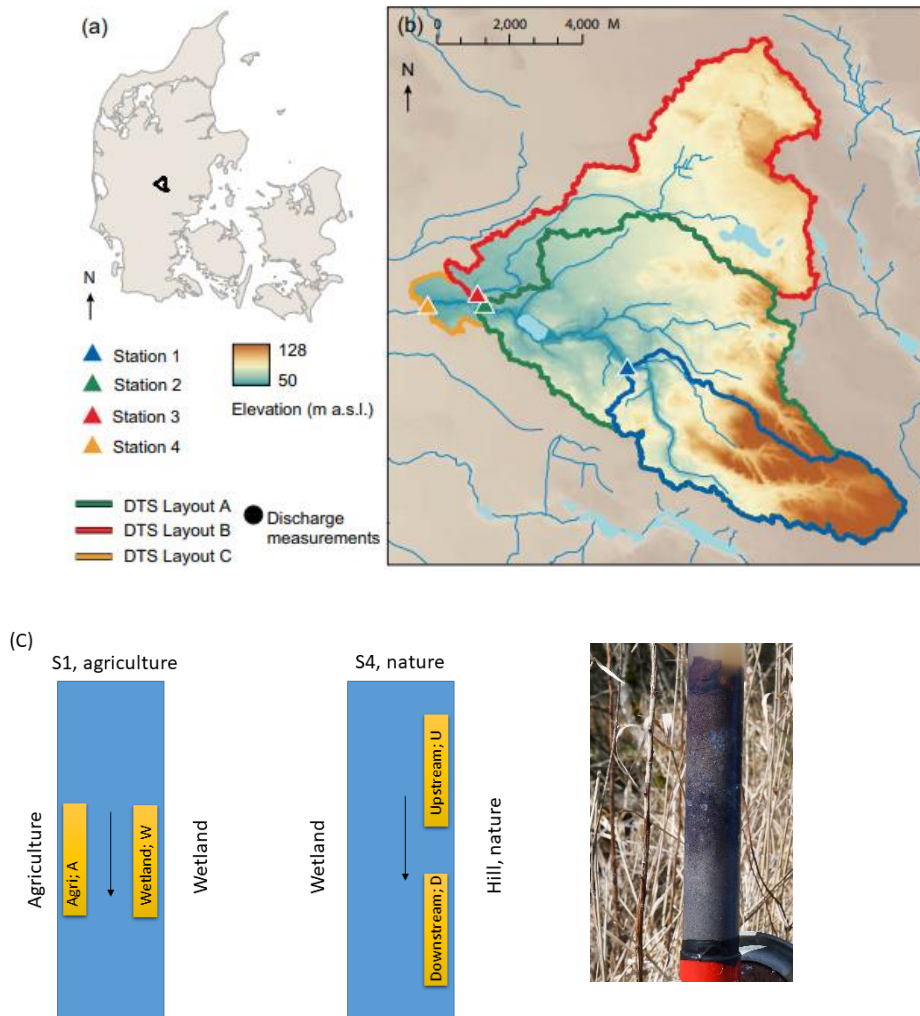


Figure 3. Overview of the different stations along the Holtum stream (A and B) (Poulsen et al. 2015). In the present study, only stations 1 and 4 were included (C), where station 1 (S1) is agriculturally impacted, and station 4 (S4) is surrounded by wetlands (C). The soil columns show the two investigated horizons from the four sampling locations (yellow squares in C), giving upper organic-rich sediment and a lower sandy sediment (photo).



Table 1 Catchment characteristics and land use for each sub-catchment, with mean annual discharge, catchment size, specific discharge, distance from the source and land use (Poulsen et al. 2015).

	<i>Mean annual discharge</i>	<i>Catchment size</i>	<i>Distance from the source</i>	<i>Urban</i>	<i>Agriculture</i>	<i>Forest</i>
	$\text{m}^3 \text{s}^{-1}$	$\text{km}^2$	m	%		
Station 1	0.17	26	6.6	27	51	20
Station 2	0.8	70	12.7	21	56	22
Station 3	0.28	42	11.6	16	41	41
Station 4	1.2	114	14.7	13	53	34

## 2.4 Planned work at each site

Figure 4 provides an overview of the planned work at each site, including the effect of organic carbon, redox conditions, pH, and temperature on contaminant degradation and mineralization. Complete mineralization was determined from microcosm studies with sediments and water using  $^{14}\text{C}$  labeled pollutants. Degradation rates ( $\text{DT}_{50}$ ) were determined from microcosm studies with river sediments.

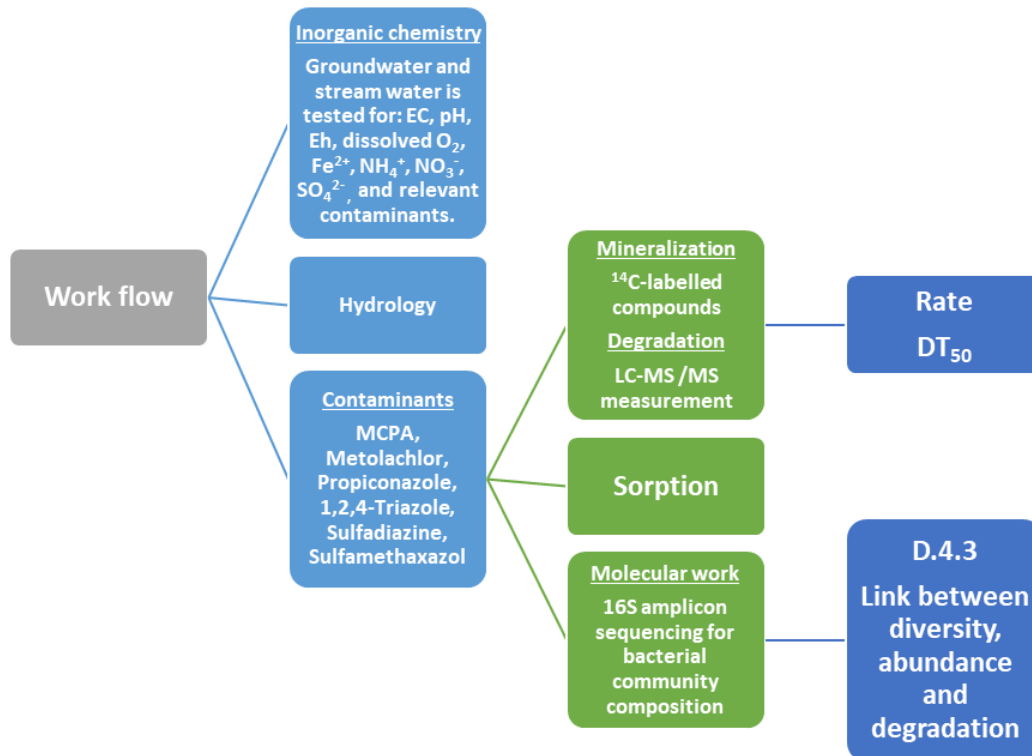


Figure 4. Overview of the planned work at each of the three sites. The link between diversity, abundance and degradation is presented in this deliverable D4.3, and based on the given in deliverable D4.2.



### **3 BACTERIAL DIVERSITY IN TRANSITIONS ZONES – LINK TO BIODEGRADATION OF PESTICIDES**

#### **3.1 Sequencing and data analysis**

##### **3.1.1 DNA extraction**

According to the manufactures recommendations, DNA from sediment samples was extracted using the Dneasy Powersoil Kit (Qiagen) and quantified by Qubit fluorometer (Invitrogen).

##### **3.1.2 16S Quantification**

The abundance of the 16S rRNA gene in sediment samples was quantified using quantitative real-time PCR in a CFX96 real-time detection system (Bio-Rad Laboratories, Inc., Hercules, CA, USA). The gene was amplified according to (Suzuki et al., 2000) by primer pair 1369F (5'-CGGTGAATACGTTTCYCGG-3) and 1492R (5'-GGWTACCTTGTTACGACTT-3) and probe (TM1389F 5'-FAM CTTGTACACACCGCCCGTC 3'-TAMRA). A 10-fold dilution series of *E. coli* K12 DNA was used for the standard curve. PCR amplification was performed in 30  $\mu$ l reactions containing 15  $\mu$ l Lo-Rox Probe Mix (PCR Biosystems, London, UK), 1.2  $\mu$ l of both primers (100 pmol/ $\mu$ l), 0.6  $\mu$ l probe (Eurofins Genomics, Galten, Denmark), 11  $\mu$ l water and 1  $\mu$ l TC-DNA. Protocol for qPCR was 3 min at 95°C, followed by 40 cycles of 10 s at 95°C and 30 s at 60°C.

##### **3.1.3 Amplicon Sequencing**

A 2-step protocol prepared the 16S gene amplicon library. In the first PCR, the 16S gene was amplified from 515 to 926 (Quince et al., 2011; Parada et al., 2016). The PCR mix contained 10  $\mu$ l Phusion buffer mix, 0.6  $\mu$ l DMSO, 0.5  $\mu$ l reverse and forward primers, 6.4  $\mu$ l milli-Q water, and 2  $\mu$ l DNA template. The PCR program was set to 98 °C for 30 seconds initial denaturation step, followed by 30 cycles with 98 °C for 10 seconds, 55 °C for 30 seconds, and 72 °C for 30 seconds and a final elongation step at 72 °C for 10 minutes. Product purity and length was assessed using agarose gel electrophoresis. In the second PCR Illumina index barcodes were attached. The PCR mix contained 10  $\mu$ l Phusion buffer mix, 1  $\mu$ l P5 and P7 primers, 11  $\mu$ l milli-Q water, and 2  $\mu$ l PCR product from the first reaction. The temperature program was set to 98 °C for 30 seconds followed by 7 cycles with 98 °C for 10 seconds, 55°C for 30 seconds, and 72°C for 30 seconds and a final elongation step at 72 °C for 10 minutes. PCR products were verified by agarose gel. PCR products were cleaned up using a MagBio clean-up system, quantified by Qubit fluorometry and normalized before Mi-sequencing.

##### **3.1.4 Bioinformatics**

Sequences were processed on the Galaxy platform using FROGS (Escudié et al., 2018) based on the Galaxy analysis platform (Afgan et al., 2016). Sequences were demultiplexed, dereplicated, sequence quality was checked, oligonucleotides, linker, pads and barcodes were removed from sequences, and sequences were filtered on additional criteria. Sequences were removed from data set if they exhibited ambiguous bases or did not match expectations in amplicon size. Remaining sequences were clustered into OTUs based on the iterative Swarm algorithm, then chimeras and singletons (OTUs containing only one sequence) were removed. Bacterial double affiliation was performed by blasting OTUs against SILVA database (Quast et al 2013). OTUs with affiliation <100% at the phylum level were removed from the data set. OTUs at lower taxonomic



ranks than the phylum level were considered as “unidentified” below when the RDP bootstrap value was <0.70.

### **3.1.5 Statistical Analyses**

Principal component analyses were performed using R-Studio version 1.0.153 and the factoextra package.

## **3.2 River Crieu**

### **3.2.1 Water chemistry**

A principal component analysis (PCA) of the water chemistry data (Figure 5) showed three distinct water chemistry signatures between Villeneuve and Saverdun groundwaters and the surface waters along the river, explaining nearly 77% of the variability. Variables that contributed most to the first axis and separated groundwater samples from rivers samples were the anion and cation composition as well as the organic matter contents, pH and redox conditions, whereas those that contributed to separating the two lots of groundwater samples were  $O^{18}$  and conductivity, possibly higher in Saverdun samples due to groundwater upwelling. The plot reveals that all surface water samples cluster to the right and groundwater samples cluster to the left. Furthermore, Saverdun groundwater samples are in the upper left quadrant whereas Villeneuve groundwater samples are in the lower left quadrant. Interestingly, Villa differed from the other groundwater samples by being closer to the surface water samples, corroborating the hypothesis that this piezometer is impacted by the river water infiltration.

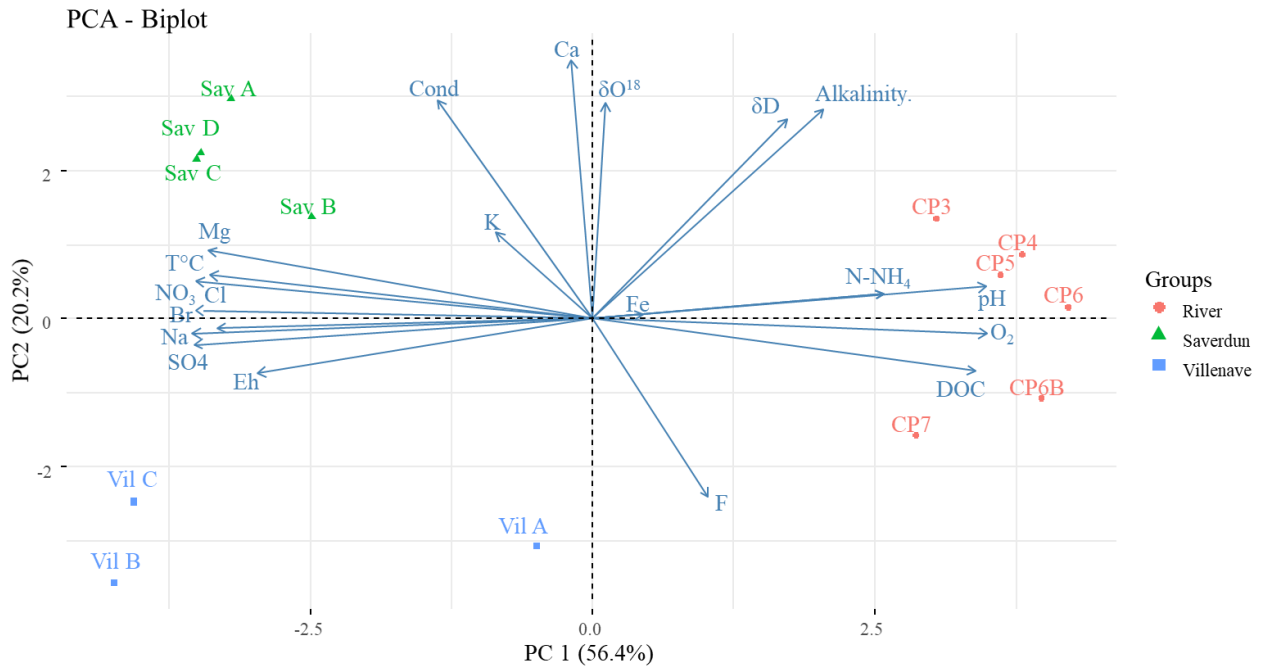


Figure 5. Biplot of a PCA analysis on the water chemistry data.

### 3.2.2 Microbial diversity analysis

Bacterial diversity was assessed using Illumina sequencing. After cleaning the raw data as described in section 3.1.4., a total of 126,786 sequences distributed among 1473 OTUs were considered. Diversity indexes (Shannon and inverse Simpson, Figure 6) did not highlight big differences between samples, although diversity appeared slightly lower in sediment CP5.

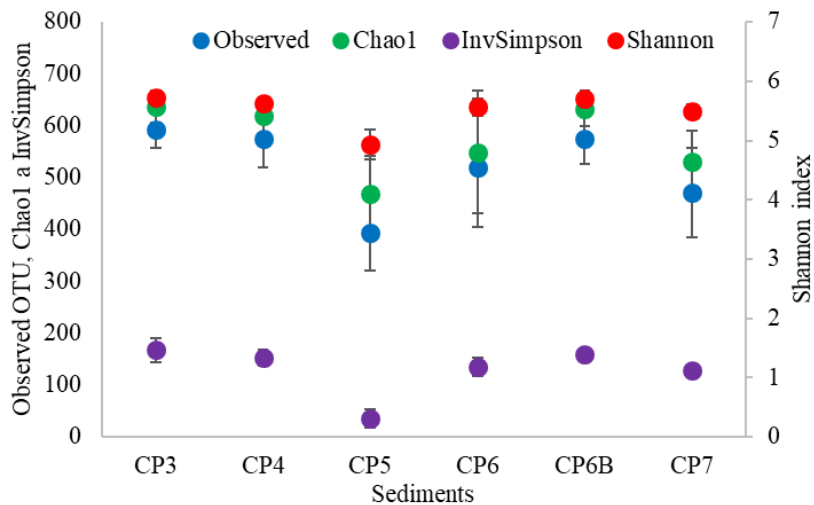


Figure 6. Diversity indexes. Error bars represent standard variation of 3 replicates.



The histogram displayed in figure 7 presents the genera or closest level of identification found in sediment samples with relative sequence abundances >1%. A first observation is that apart from CP5, where one OTU, affiliated to the *Phormidiaceae* family, represent between 10 and 15% of the relative sequence abundance, no other OTUs represent more than a small percentage of the sequences and the majority of OTUs (between 60 and 85%) represent less than 1% of the relative sequence abundance. Several OTUs were found in all samples, for example, the genus *Nitrospira*, *Pirellula* and *Tychonema*, where others are only found in one or several sediment samples, for instance, *Comomonas* in CP6A and CP7 or *Gaiella* in CP4 and CP6 (B) and CP6B (A and B), suggesting specific differences between these sediment samples.

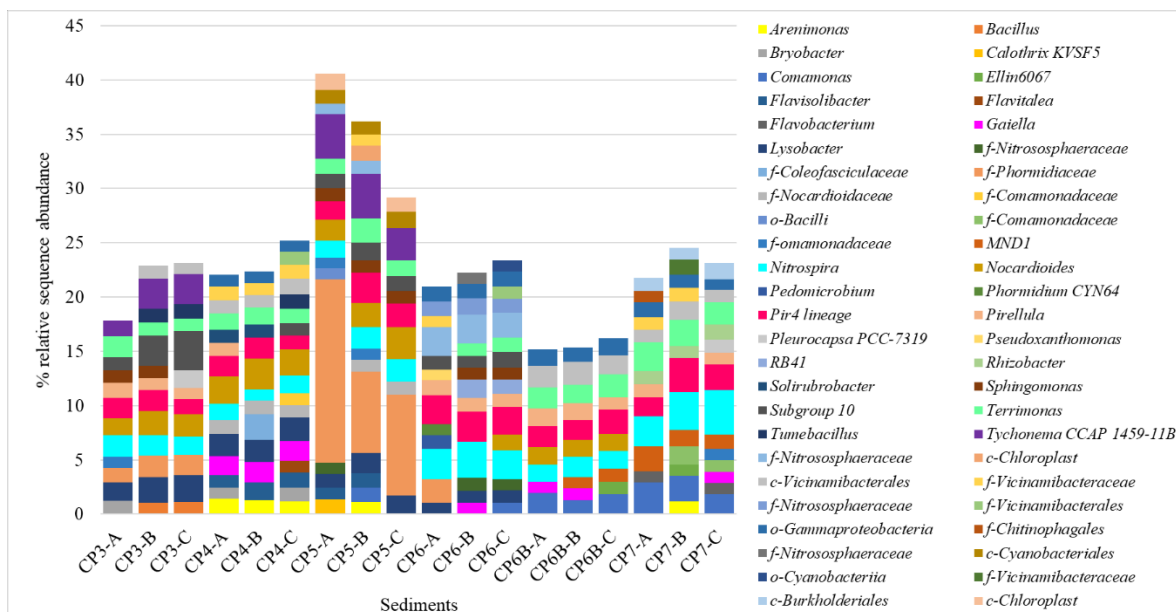


Figure 7. Histogram presenting the genera found at > 1% of the relative sequence abundance. Affiliation is given at the genus level if available or at the closest level of identification (f: family; c: class; o: order).

Furthermore, in figure 8, representing a biplot of a PCA analysis of the genera representing >0.5% sequences, the first two axes of this analysis explain 35% of the data variability and show that replicates of the same sediments cluster together, indicating little variation, whereas it highlights differences between sediments. In particular, CP6B and CP7 cluster together at the right of the biplot, whereas CP3, CP4 and CP5 cluster to the left. CP6 is further separated from the other samples along the second axis. Projected on this plot are the 30 variables (OTUs) that explain the most this distribution (not necessarily the most abundant) and could be linked to specific differences between sediment samples, as previously highlighted for the water chemistry.

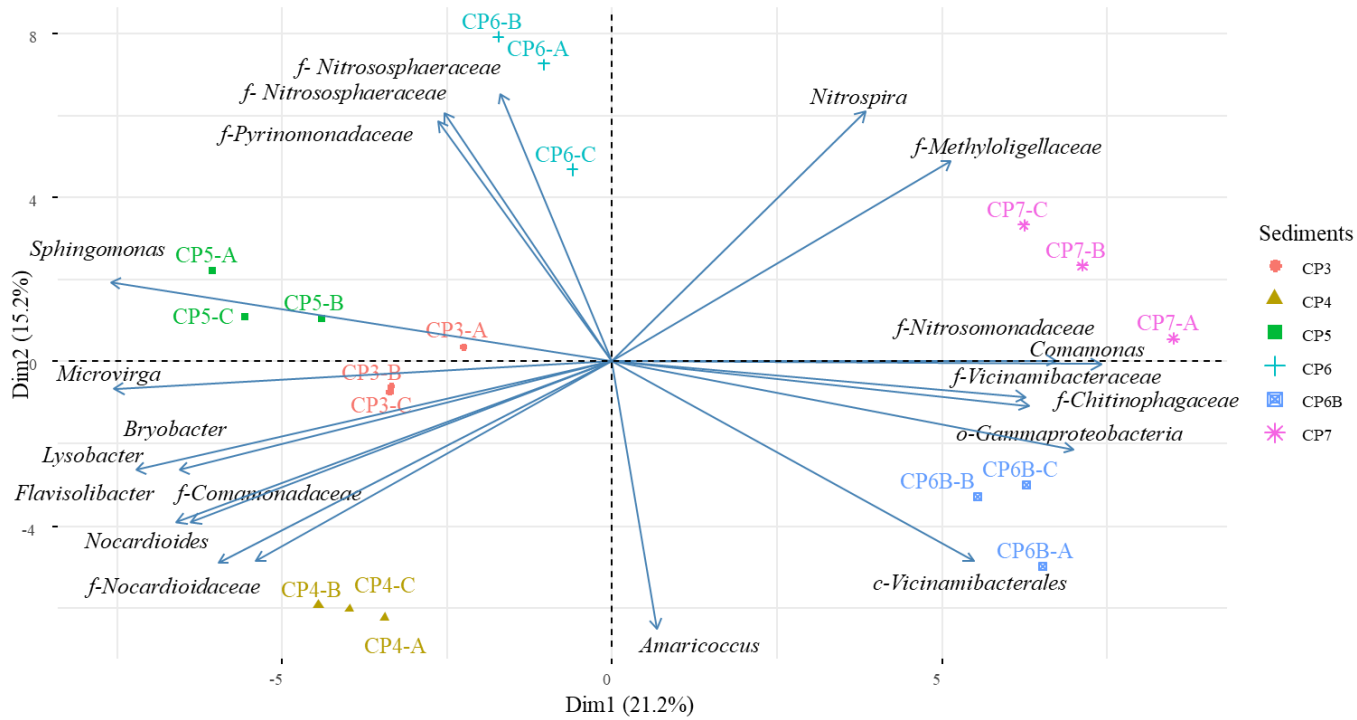


Figure 8. Biplot of a PCA analysis of the genera representing > 0.5% sequence relative abundance. Projected arrows correspond to 30 variables that contribute the most to the data distribution.

### 3.3 Risby stream

#### 3.3.1 Diversity analysis

Bacterial diversity was assessed using Illumina sequencing. After cleaning the raw data as described in section 3.1.4., a total of 901,482 sequences distributed among 1375 OTUs were considered. Diversity indexes (Shannon and inverse Simpson, Figure 9) did not highlight big differences between samples for the A horizon samples, with around 750 observed OTUs and a Shannon index between 5 and 6, whereas diversity indexes were lower for the deeper sediment samples (C horizon), especially for C1 (Site 1) and C3 (Site 3) with 650 and 520 observed OTUs, respectively.

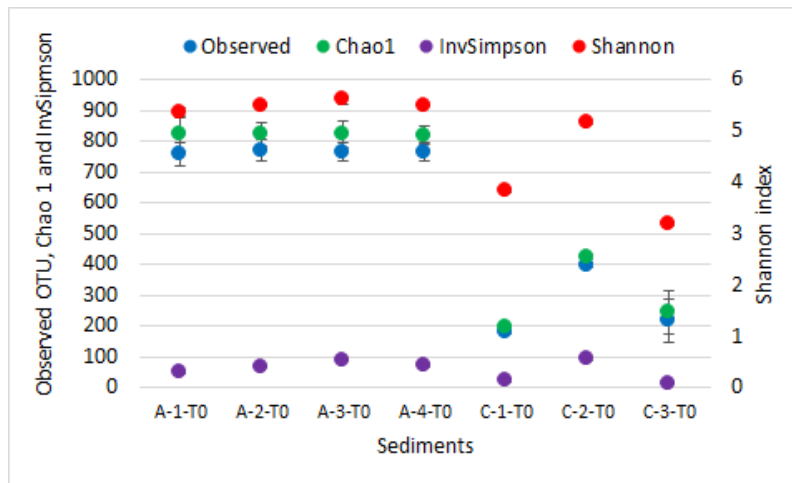


Figure 9. Diversity indexes. Error bars represent standard variation of 3 replicates.

Figure 10 presents a histogram of the genera that represent more than 1% of the relative sequence abundance. As for the diversity indexes, the diversity profiles for these genera are very similar for all four A horizon samples with three taxa that stand out, one from the order of *Vicinamibacteria*, one from the *Steroidobactereceae* family and one from the *Comamonadaceae* family. On the other hand, diversity was more different between samples from the deeper C horizon. In C1 samples the *Comamonadaceae* family was the taxa with the most relative sequence abundance followed by the genera *Pseudomonas*, *Sideroxydans*, *Gallionella* and *Sulfuricurvum*, known as iron and sulfur oxidizing taxa. In C2 the taxa representing the most relative sequence abundance are from the order *Vicinamibacteria* and genera *Flavobacterium*, *Candidatus Methylophilus* and *Fluviicola* whereas in C3 the replicates differ, C3-a containing highest abundances of the family *Lachnospiraceae* and the genera *Paludibacter* and *Pelosinus*, in common with C3-b and c there is a *Clostridium sensu stricto 1* but then these samples were dominated by *Pseudomonas*, *Herminiimonas*, and the *Comamonadaceae* and *Oxalobacteraceae* families.

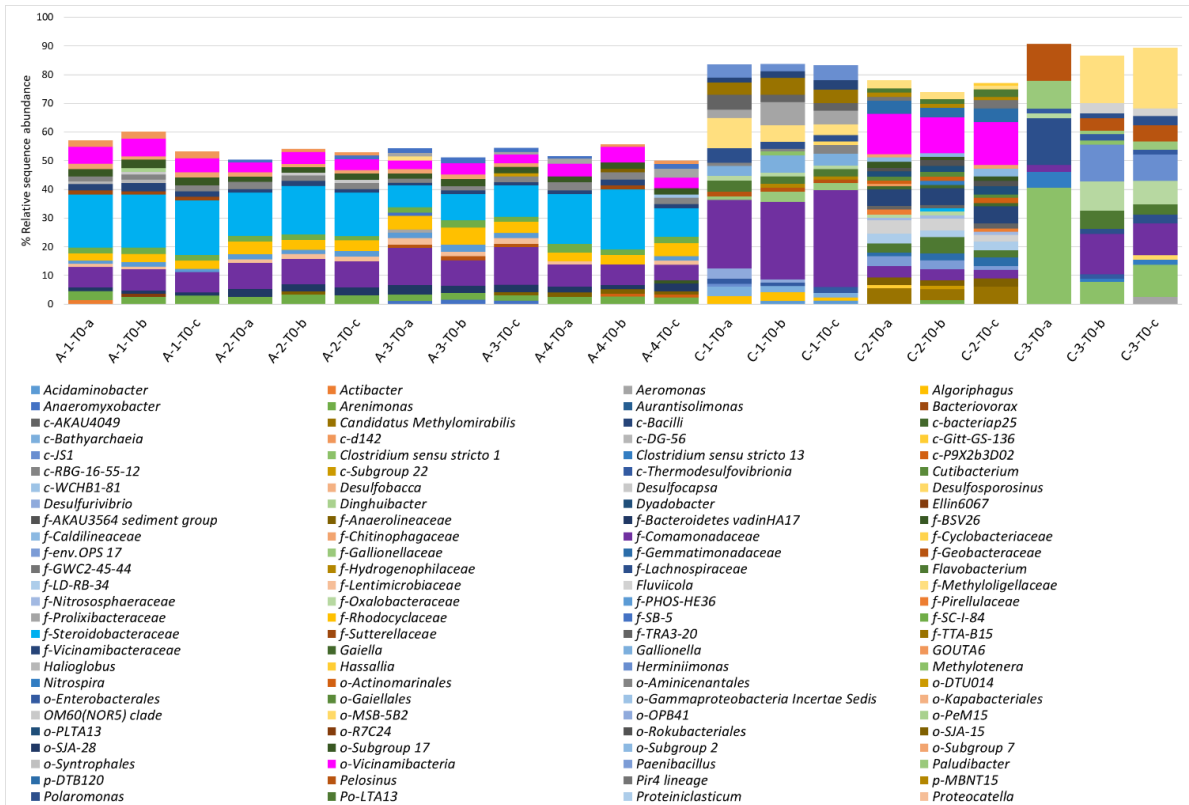


Figure 10. Histogram presenting the genera found at > 1% of the relative sequence abundance. Affiliation is given at the genus level if available or at the closest level of identification (f: family; c: class; o: order).

A PCA analysis of the sequencing data is presented in figure 11. This confirms differences between C and A samples although C2 clusters with the A samples. The variables that contribute the most to explaining these differences are the dominant ones found in each sample and highlighted in the previous paragraph.

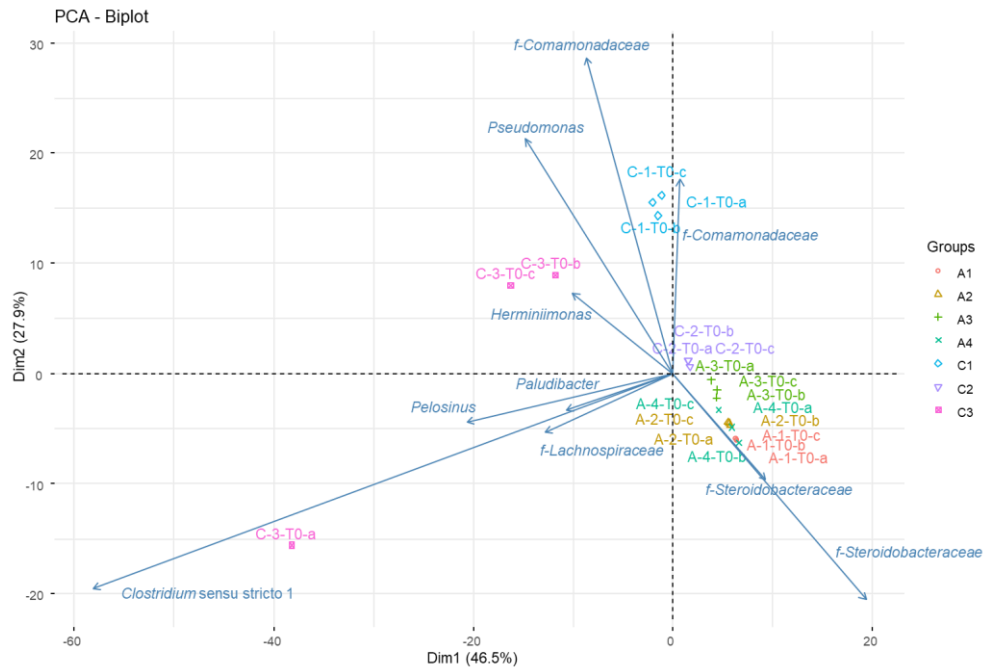


Figure 11. Biplot of a PCA analysis of the genus representing > 0.5% sequence relative abundance. Projected arrows correspond to 30 variables that contribute the most to the data distribution.

### 3.3.2 Evolution of diversity profiles after 100 days incubation

As presented in D4.2., samples from the Risby site were incubated either in aerobic (A horizon) or anaerobic (C horizon) conditions to monitor pesticide degradation. For the Risby site incubations, DNA extractions and sequencing were also carried out after 100 days incubation. The diversity results are presented in figure 12 as histograms, for the A and C horizons, of the genera represented by >1% of the relative sequence abundance. For the A horizon, incubated in aerobic conditions, the diversity observed after 100 days was very similar to the initial diversity (Figure 12, upper panel). On the other hand, in the C horizon samples, incubated in anaerobic conditions, several taxa increased at the stake of the previously dominant taxa. In C1 and C2, sulfate reducing taxa such as *Desulfosoposinus* and the order of *Desulfitobacterium* increased whereas in C3 the incubation conditions favored the genus *Sedimentibacter* and *Acetobacterium* (Figure 12, lower panel).

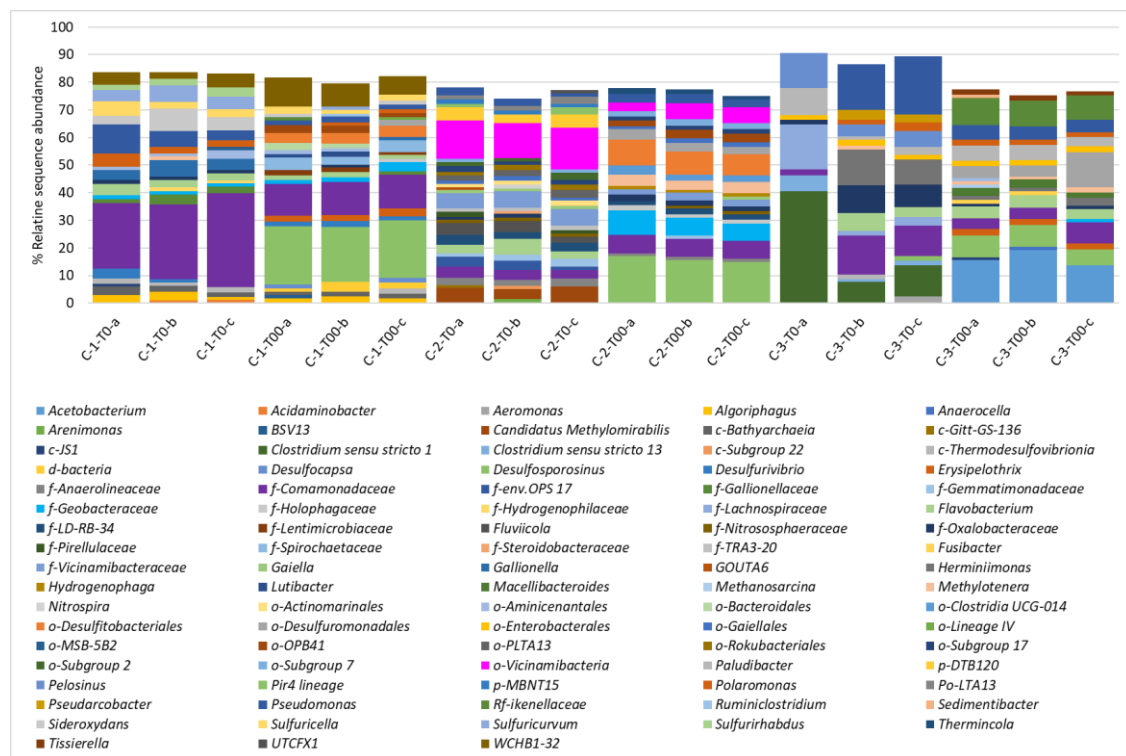
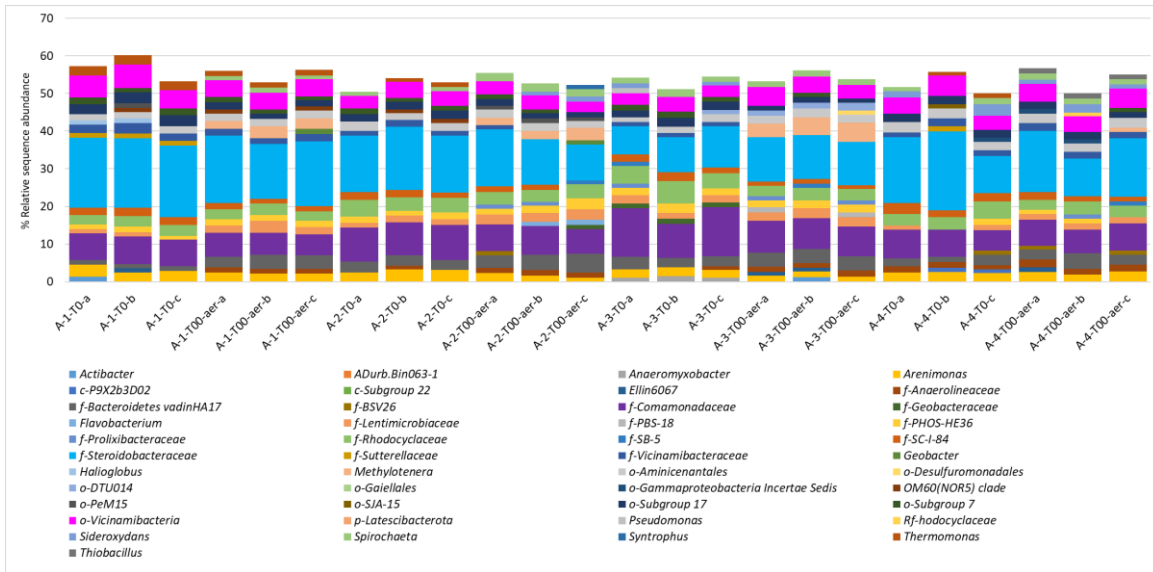


Figure 12. Histogram presenting the genera found at > 1% of the relative sequence abundance. Affiliation is given at the genus level if available or at the closest level of identification (f: family; c: class; o: order). Upper panel: Aerobic samples (A-horizon) after incubation for 100 days at aerobic conditions. Lower panel: Anaerobic samples (C-horizon) after incubation for 100 days at anaerobic conditions.



### 3.4 Holtum stream

#### 3.4.1 Water chemistry

Holtum stream water and drain water from the agricultural field adjacent to the river as well as pore waters from the riverbed sediments were sampled and analyzed for geochemical parameters such as dissolved organic carbon (DOC),  $\text{SO}_4^{2-}$ ,  $\text{HCO}_3^-$ ,  $\text{NO}_3^-$ ,  $\text{NH}_4^+\text{-N}$  and  $\text{Cl}^-$  and analyzed by PCA (figure 13). These results highlight in particular differences for the Station 1 pore water samples due to the  $\text{NH}_4^+\text{-N}$  and  $\text{Cl}^- / \text{SO}_4^{2-}$  contents although as described below, these differences did not appear to influence differences in diversity.

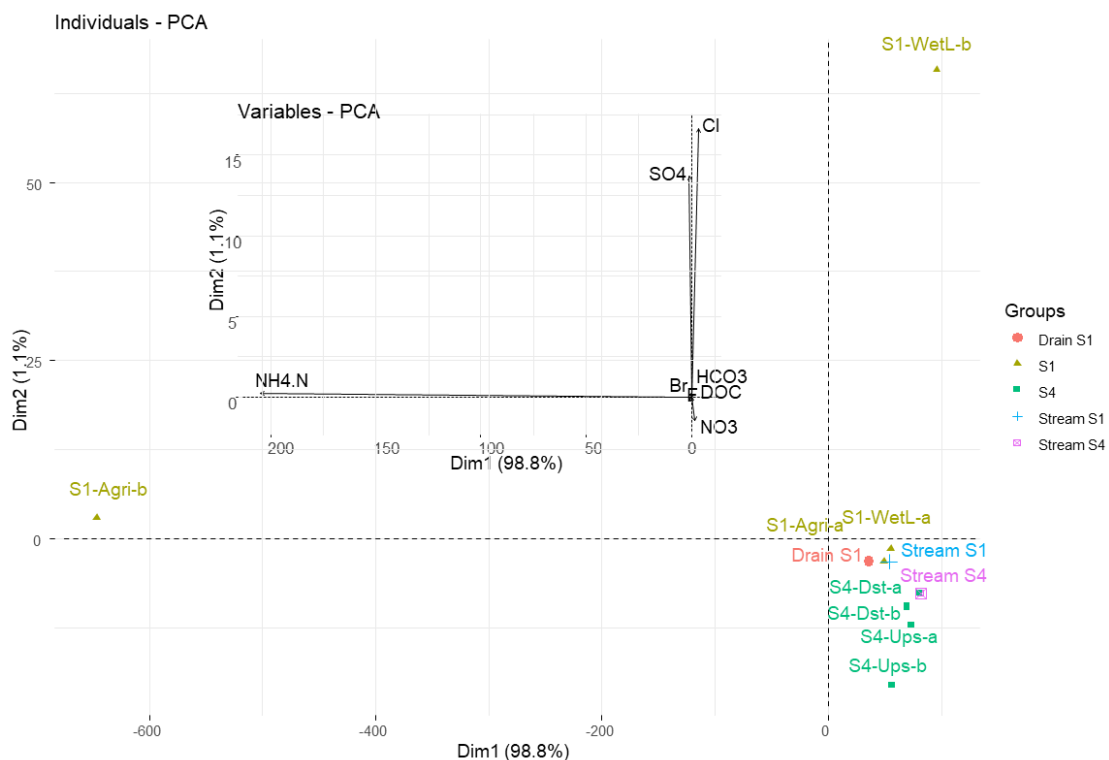


Figure 13. Biplot of a PCA analysis on the water chemistry data.

#### 3.4.2 Diversity analysis

Holtum stream consists of sediment samples collected from two stations, Station 1 (agricultural) and Station 4 (natural). At each Station, two situations were considered: for Station 1 the agricultural and the wetland sides of the stream (S1-Agri and S1-WetL, respectively), and for Station 4, an upstream and downstream point (S4-Ups and S4-Dst, respectively). At each sampling point, intact sediment cores were sampled and divided into two sections (A-horizon, 10-15 cm, B-horizon 15-30 cm). At each of these 4 sampling points, 4 samples were collected for each horizon and DNA was extracted from 3 subsamples of these, resulting in 12 extractions for each sampling point and horizon. Replicability of the extractions and diversity was checked with the 3 subsamples and for clarity in this report data are presented either as the means of 12 analyses or of three when all four samples are considered (further named “sediment columns”).



After cleaning the raw data as described in section 3.1.4., a total of 4,635,737 sequences distributed among 2109 OTUs were considered for further analysis. Diversity indexes (Figure 14 showed a lower number of observed and calculated (Chao1) OTUs in the B horizon samples than the A-horizon ones at three of the sampling points (S1-Agri, S4-Ups and S4-Dst). This explains the decrease in the Shannon and inv-Simpsons index for the replicate samples.

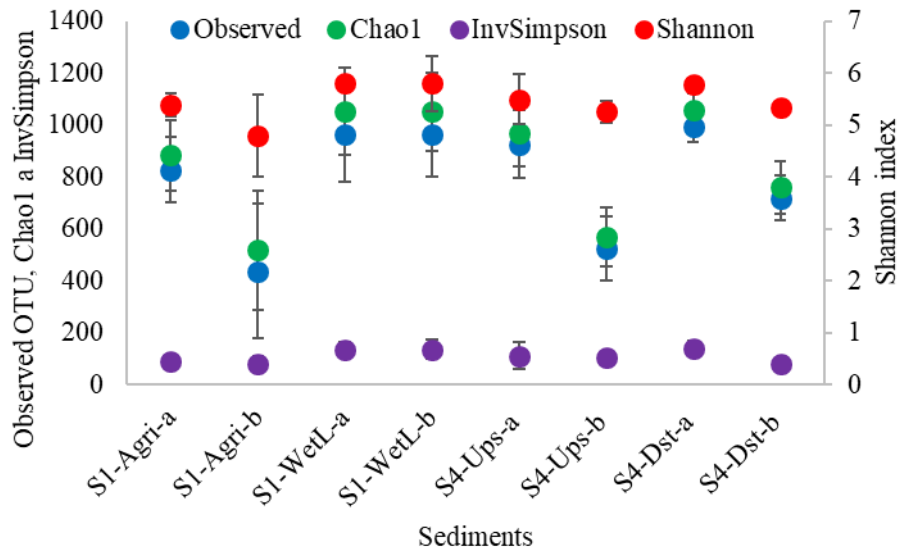


Figure 14. Diversity indexes. Error bars represent standard variation of 12 replicates.

As for the previous sites, a histogram of the genera that represent >1% of the relative sequence abundance is presented in figure 15. This figure shows that when considering these genera, the 4 samples collected for each sampling point (columns C1-C4) are very similar. It also underlines similarities between the A and B horizons of the four sites but also several genera which are more abundant at Station 1 than station 4 or vis-versa, for example, o-subgroup 2, which is affiliated to the class of *Acidobacteriae*; *Candidatus*, *Methylomirabilis*, and OTU affiliated to the order of *o-Rokubacteriales* are only present at >1% relative sequence abundances at Station 4.

OTU with the highest relative abundance belong to few taxonomical groups, several iron oxidizing taxa (*Sideroxydans*, *Gallionella*), *Candidatus* *Methylomirabilis*, that can couple anaerobic methane oxidation with nitrite reduction in anoxic environments, *Thermodesulfovibrionia*, a denitrifying bacterium, or *Rokubacteriales*, an order containing nitrate reducing species.

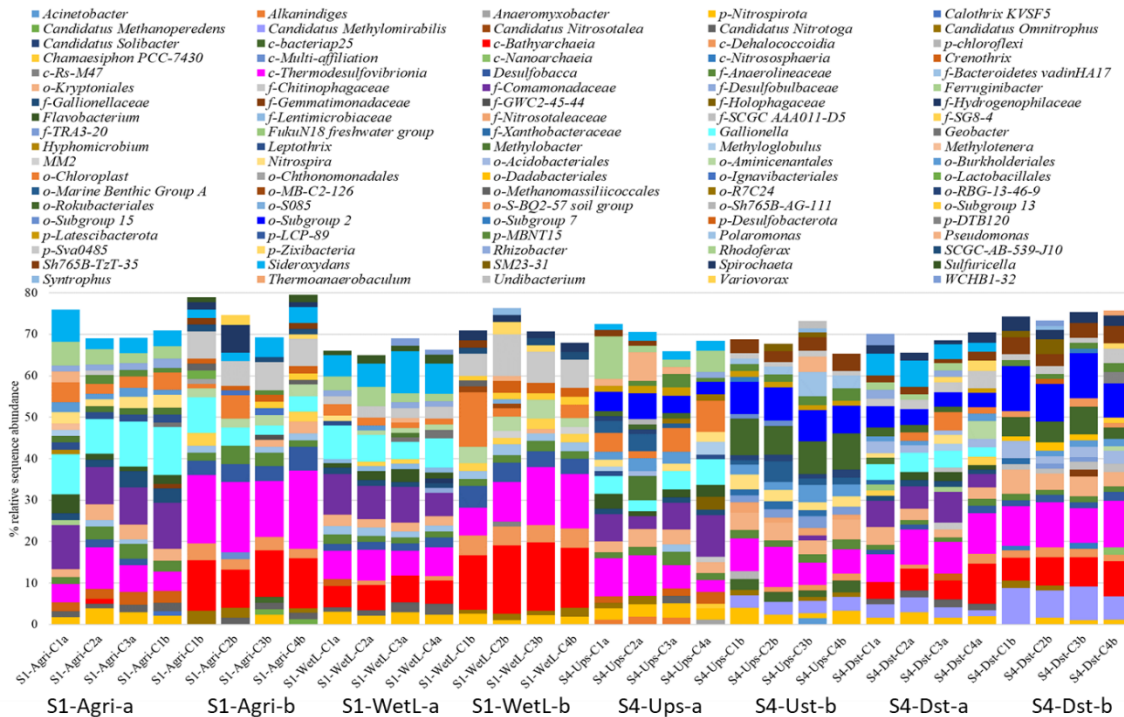


Figure 15. Histogram presenting the genera found in the sediment samples at >1% relative abundance. Affiliation is given at the genus level if available or at the closest level of identification (f: family; c: class; o: order).

In agreement with the histogram in figure 15, which suggests similarities, for the most abundant OTUs, between the A and B horizons for the four sampling points, a PCA analysis (Figure 16) grouped the sampling sites according to the horizon and the station. For both stations, the A and B horizons are separated along the second axis (PC2, 21.4% data variability). In contrast, the two stations are more separated along the first axis (PC1, 23.2% data variability), due in particular to *Candidatus MethyloMirabilis*, a genus absent from Station 1. These differences could, in part, be linked to physico-chemical conditions; indeed, denitrifiers would require more reductive conditions that are possibly found in the lower B-horizons compared to A.

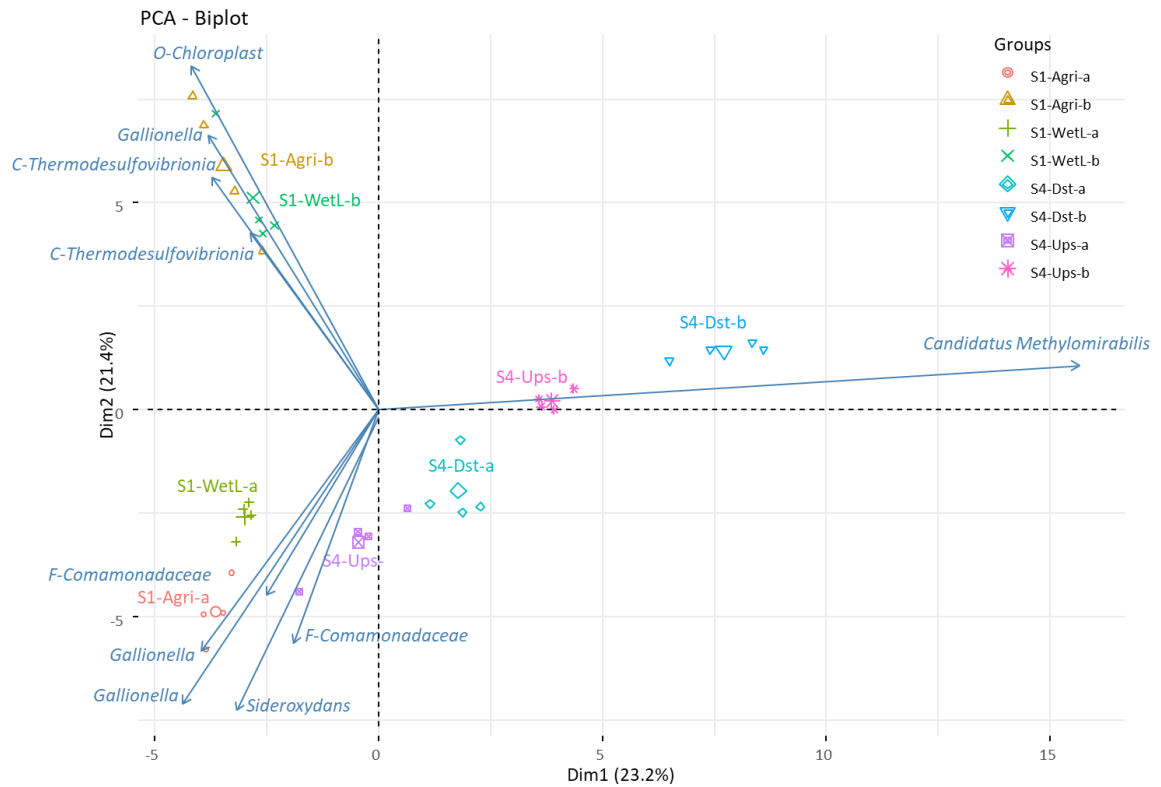


Figure 16. Biplot of a PCA analysis of the diversity data. Projected arrows correspond to 10 variables that contribute the most to the data distribution.



## 4 DISCUSSION – LINKING DIVERSITY AND DEGRADATION RATES IN SEDIMENT TRANSITION ZONES

### 4.1.1 Sediment diversity and DT50 for MCPA, metolachlor and propiconazole

As described in D4.2, degradation kinetics varied in the different sediment samples as assessed with the DT values, representing the time (days) required to degrade one half of the contaminant. These data are presented for the three sites in table 2. The Crieu river and Risby sediments demonstrated the best ability to degrade MCPA and metolachlor, while propiconazole was not degraded by the microbial consortia present in the Risby sediments. On the other hand, the Holtum sediments showed the slowest degradation for the two measured compounds, MCPA and metolachlor, with a minimum of 90 and 107 days before reaching 50% degradation, respectively

Table 2. DT50 values measured in the sediments for MCPA, metolachlor and propiconazole. Depending on the degradation profiles, DTs were calculated from first order models (Crieu and Risby) or from linear regression. Values represent means of 3 replicates. For more details, please refer to D4.2.

DT50			
Crieu	MCPA	Metolachlor	Propiconazole
CP3	22.1	15.9	74.8
CP4	11.1	24.0	146.5
CP5	27.4	11.5	94.7
CP6	1.2	14.4	59.8
CP6B	5.3	44.8	108.2
CP7	12.0	35.2	89.8
DT50			
Risby	MCPA	Metolachlor	Propiconazole
SM1	10.0	18.0	not degraded
SM2	6.5	21.8	
SM3	6.1	42.4	
SM4	8.2	40.9	
DT50			
Holtum	MCPA	Metolachlor	Propiconazole
S1-Agri-a	107.5	107.5	not measured
S1-Agri-b	466.8	374.0	
S1-WetL-a	144.2	107.2	
S1-WetL-b	261.2	1393.8	
S4-Ups-a	213.3	90.1	
S4-Ust-b	148.9	1380.0	
S4-Dst-a	slow	96.2	
S4-Dst-b	272.2	208.5	



The question addressed here is whether we can link these DT50 values to a specific diversity?

MCPA degradation is initiated with a first step carried out by an  $\alpha$ -ketoglutarate-dependent dioxygenase encoded by *tfdA* or *tfdA* like genes detected in proteobacteria (Batioğlu-Pazarbaşı et al. 2013). Previous research has found significant presence of these genes in soils (Mierzejewska et al. 2018), suggesting a rather ubiquitous function, unrelated to a specific bacterial genus. Metolachlor has been shown to be degraded, in particular by *Bacillus* sp. in aerobic conditions and bacteria affiliated to the Acidobacteria phylum by Kanissery et al. (2018), who used DNA-stable isotope probing to identify metolachlor degraders. These authors remind us that to date, no microorganisms that degrade metolachlor have been isolated. Propiconazole, a fungicide, has been shown to be degraded by *Pseudomonas aeruginosa* (Satapute & Kaliwal 2016b) and by an isolated strain of *Burkholderia* sp. (Satapute & Kaliwal 2016a).

The bacterial diversity measured here using Illumina sequencing shows diverse communities in all the sediments from the three sites. Several taxa can be found in most sediments such as the *comamonadaeae* family and iron oxidizers such as *Gallionella* and *Sideroxydans* genera and linked to physico-chemical conditions. Overall diversity was lower in the Crieu river sediments although these were the ones where degradation rates were fastest, maybe these sediments are more exposed to these components than the Holtum and Risby ones which would explain this. However, based on the global microbial diversity analysis, it was not possible to link a specific diversity pattern to a degradation potential for these compounds.

#### **4.1.2 Sediment diversity and degradation of antibiotics and two other pesticides, metamitron and pyrastrubin, in the Holtum stream sediments**

Another family of emerging contaminants, antibiotics, was tested for degradation in the Holtum sediments and, as for the pesticides, DT50s were assessed and results presented in D4.2. In addition, two more pesticides were included in the Holtum experiment that revealed simple first order degradation kinetics, and hence it was possible to calculate DT50 values for metamitron and pyrastrubin. DT50s values for these compounds are presented in table 3. The two sulfonamides were degraded relatively quickly, especially in the top horizons with DT50 values ranging from 9.4 to 20.5 days. Detected values for the top horizons are in accordance with other studies where half-life (DT50) of sulfamethoxazole in the top layer of an agricultural soil in Shanghai, here, sulfamethoxazole (20 mg/kg) was found to have a DT50 of 10.8 days (Zhang et al. 2017). In a loam and a loamy-sand manure-amended soil, half-life of sulfamethoxazole was of 5.4 and 15 days respectively (Wu et al. 2012). In three different pasture soils, under biotic conditions, DT50 values were found to be 9.2, 4.3 and 13.3 days (Srinivasan & Sarmah 2014). Pure cultures can degrade sulfamethoxazole by metabolism and cometabolism, where known degraders includes: *Acinetobacter* sp., *Microbacterium* sp., *Achromobacter denitrificans* strain PR1, *Rhodococcus equi* (Wang & Wang 2018). Kassotaki et al. (2016) also linked sulfamethoxazole degradation to co-metabolism involving ammonia oxidizers. Potential sulfadiazine degraders have been suggested in agricultural soil; *Gaiella*, *Clostridium sensu stricto\_1*, *Tumebacillus*, *Roseiflexus*, *Variocorax*, *Nocardioide* and *Bacillus*, where degradation essays measured DT50s of 0.96–2.57 days (Chen et al. 2019). For metamitron DT50 values ranged from 18.8 to 56.3 in agricultural soils which is in the similar range of this study for both the upper horizon and the lower horizon (Vischetti et al. 1997) but no specific degraders have been identified to our best knowledge. The fungicide pyraclostrobin was found to have a DT50 value of ~60 in an agricultural soil, which is slightly slower than in the



top horizon, but faster than the lower horizon (Fulcher et al. 2014). Only a few studies on biodegradation of strobilurins have been reported in the literature including a pyraclostrobin-degrader *Klebsiella sp.* from soybean-grown soil after long-term use of this pesticide, and two *Pseudomonas* strains (*Burkholderia* and *Pseudomonas aeruginosa*) were isolated from pyraclostrobin-contaminated natural environment, which were capable of degrading pyraclostrobin and azoxystrobin (Chen et al. 2018).

Table 3. DT50 values calculated for sulfadiazine, sulfametoxazole, metamitron and pyrastrubin in Holtum sediments. DT50s values were calculated from first order models. Values represent means of 3 replicates. For more details, please refer to D4.2.

Holtum	DT50			
	Sulfadiazine	Sulfametoxazole	Metamitron	Pyrastrubin
<b>S1-Agri-a</b>	13.7	10.8	23.0	21.5
<b>S1-Agri-b</b>	18.4	23.5	42.2	633.7
<b>S1-WetL-a</b>	15.9	9.4	13.0	22.4
<b>S1-WetL-b</b>	20.5	36.5	51.0	320.2
<b>S4-Ups-a</b>	14.8	13.8	15.5	22.3
<b>S4-Ups-b</b>	43.4	92.7	52.8	32.3
<b>S4-Dst-a</b>	20.5	14.8	33.8	28.4
<b>S4-Dst-b</b>	16.4	27.3	76.9	45.1

As for the previous compounds, although several OTUs could be affiliated to genera that have been shown to degrade these compounds, without further exploration of the data from a metabolic point of view and possibly the acquisition of data on the presence and quantification of a degradation potential, for example by quantifying specific gene abundances, it is not presently possible to conclude on a specific diversity profile that would guarantee the degradation of these compounds in river sediments.

#### 4.1.3 Conclusion

The differences observed in the DT50 values cannot solely be explained by the 16S amplicon sequencing at any of the three sites. Further analysis of the diversity data to link the profiles to potential metabolisms could help identify specific patterns that contribute to enhancing degradation but, here, without the specific demarcation of known pesticide degraders it is not possible to conclude on bacterial markers of degradation potentials. However several interesting points have been highlighted through this work, in particular

- The strong variability between DT50 in the different sediments, showing that although we presently cannot link them to a specific diversity profile, the bacteria capable of degrading these compounds are not always present which could lead to errors in fate prediction of these compounds if DT50s are not systematically measured.
- An emerging common core of OTUs among sediments originating from different geographical environments for which further analysis of the data may help to pinpoint less visible differences that could explain the differences between DT50s.



## 5 REFERENCES

- Amalric L, Baran N, Coureau C, Maingot L, Buron F, Routier S (2013) Analytical developments for 47 pesticides: first identification of neutral chloroacetanilide derivatives in French groundwater. *International Journal of Environmental Analytical Chemistry* 93(15): 1660-1675.
- Batioğlu-Pazarbaşı M, Milosevic N, Malaguerra F, Binning PJ, Albrechtsen H-J, Bjerg PL, Aamand J (2013) Discharge of landfill leachate to streambed sediments impacts the mineralization potential of phenoxy acid herbicides depending on the initial abundance of *tfdA* gene classes. *Environmental Pollution* 176: 275-283.
- Chen J, Jiang X, Tong T, Miao S, Huang J, Xie S (2019) Sulfadiazine degradation in soils: Dynamics, functional gene, antibiotic resistance genes and microbial community. *Science of The Total Environment* 691: 1072-1081.
- Chen X, He S, Liang Z, Li QX, Yan H, Hu J, Liu X (2018) Biodegradation of pyraclostrobin by two microbial communities from Hawaiian soils and metabolic mechanism. *Journal of Hazardous Materials* 354: 225-230.
- Fulcher JM, Wayment DG, White PM, Webber CL (2014) Pyraclostrobin Wash-off from Sugarcane Leaves and Aerobic Dissipation in Agricultural Soil. *Journal of Agricultural and Food Chemistry* 62(10): 2141-2146.
- Houmark-Nielsen M (1989) The last interglacial-glacial cycle in Denmark. *Quaternary International* 3-4: 31-39.
- Kanissery RG, Welsh A, Gomez A, Connor L, Sims GK (2018) Identification of metolachlor mineralizing bacteria in aerobic and anaerobic soils using DNA-stable isotope probing. *Biodegradation* 29(2): 117-128.
- Kassotaki E, Buttiglieri G, Ferrando-Climent L, Rodriguez-Roda I, Pijuan M (2016) Enhanced sulfamethoxazole degradation through ammonia oxidizing bacteria co-metabolism and fate of transformation products. *Water Research* 94: 111-119.
- Mierzejewska, E. , Baran, A. , Urbaniak, M. 2018The influence of MCPA on soil ecotoxicity and the presence of genes involved in its biodegradation. *Archives of Environmental Protection*. Vol. 44, no. 4, 58-64.
- Posselt M, Mechelke J, Rutere C, Coll C, Jaeger A, Raza M, Meinikmann K, Krause S, Sobek A, Lewandowski J, Horn MA, Hollender J, Benskin JP (2020) Bacterial Diversity Controls Transformation of Wastewater-Derived Organic Contaminants in River-Simulating Flumes. *Environmental Science & Technology* 54(9): 5467-5479.
- Poulsen JR, Sebok E, Duque C, Tetzlaff D, Engesgaard PK (2015) Detecting groundwater discharge dynamics from point-to-catchment scale in a lowland stream: combining hydraulic and tracer methods. *Hydrol. Earth Syst. Sci.* 19(4): 1871-1886.
- Satapute P, Kaliwal B (2016a) Biodegradation of propiconazole by newly isolated *Burkholderia* sp. strain BBK\_9. *3 Biotech* 6(1): 110-110.
- Satapute P, Kaliwal B (2016b) Biodegradation of the fungicide propiconazole by *Pseudomonas aeruginosa* PS-4 strain isolated from a paddy soil. *Annals of Microbiology* 66(4): 1355-1365.
- Sobczak WV, Findlay S (2002) Variation in bioavailability of dissolved organic carbon among stream hyporheic flowpaths. *Ecology* 83(11): 3194-3209.
- Srinivasan P, Sarmah AK (2014) Dissipation of sulfamethoxazole in pasture soils as affected by soil and environmental factors. *Science of The Total Environment* 479-480: 284-291.
- Storey RG, Fulthorpe RR, Williams DD (1999) Perspectives and predictions on the microbial ecology of the hyporheic zone. *Freshwater Biology* 41(1): 119-130.



- 
- Vischetti C, Marucchini C, Leita L, Ceccon P, Giovanardi R (1997) Soil behaviour of metamitron in laboratory and lysimeter studies. *Agronomie* 17(8): 367-373.
- Wang J, Wang S (2018) Microbial degradation of sulfamethoxazole in the environment. *Applied Microbiology and Biotechnology* 102(8): 3573-3582.
- Wu Y, Williams M, Smith L, Chen D, Kookana R (2012) Dissipation of sulfamethoxazole and trimethoprim antibiotics from manure-amended soils. *Journal of Environmental Science and Health, Part B* 47(4): 240-249.
- Zhang Y, Hu S, Zhang H, Shen G, Yuan Z, Zhang W (2017) Degradation kinetics and mechanism of sulfadiazine and sulfamethoxazole in an agricultural soil system with manure application. *Science of The Total Environment* 607-608: 1348-1356.